CMOS-Compatible ALD Zinc Oxide Coating for On-Chip Second-Order Nonlinear Optical Functionalities

Artur Hermans[1,2], Michiel Van Daele[3], Clemens Kieninger[4,5], Jolien Dendooven[3], Stéphane Clemmen[1,2], Christophe Detavernier[3], Christian Koos[4,5], Roel Baets[1,2]

[1]*Photonics Research Group, Ghent University - imec, 9052 Ghent, Belgium*
[2]*Center for Nano- and Biophotonics, Ghent University, 9052 Ghent, Belgium*
[3]*Department of Solid State Sciences, Ghent University, 9000 Ghent, Belgium*
[4]*Institute for Microstructure Technology, Karlsruhe Institute of Technology, 76344 Eggenstein-Leopoldshafen, Germany*
[5]*Institute of Photonics and Quantum Electronics, Karlsruhe Institute of Technology, 76131 Karlsruhe, Germany*
artur.hermans@ugent.be

Abstract: We report on the atomic layer deposition of ZnO for interfacing with existing Si_3N_4 photonics which lacks 2nd-order nonlinear functionalities. We measure a $\chi^{(2)}$ of 15 pm/V in line with a bulk ZnO crystal.

OCIS codes: (160.4330) Nonlinear optical materials; (190.2620) Harmonic generation and mixing; (310.6860) Thin films, optical properties

Second-order nonlinear optical effects are at the heart of many applications: electro-optic modulators [1] and optical parametric oscillators [2] are two prominent examples. Most second-order nonlinear ($\chi^{(2)}$) devices rely on bulk nonlinear crystals or low contrast waveguides. However, the continuing expansion of silicon and silicon nitride photonics requires the intrinsically missing $\chi^{(2)}$ nonlinearity to be introduced in a way compatible with CMOS fabrication. Recent studies have pointed out atomic layer deposition (ALD) as a very promising technique to fabricate $\chi^{(2)}$ materials suitable for integration with CMOS-compatible photonic integrated circuits. Examples include the reports on ALD ABC-type nanolaminates [3,4] and ZnO nanolaminates [5]. ALD is an attractive technique because it is a low-temperature, conformal deposition process that works on a large variety of substrates and provides thickness precision at the monolayer level. In this paper, we report on the $\chi^{(2)}$ nonlinearities of plasma-enhanced ALD (PE-ALD) ZnO thin films on amorphous glass substrates which are found to be significantly larger than those observed for thermal ALD ZnO [5]. ZnO is a wide band gap material (~3.3 eV) that crystallizes preferably in the hexagonal wurtzite structure, point group 6mm [6]. For ZnO single crystals, $\chi_{zzz} = -14.31$ pm/V and $\chi_{zxx} = 1.36$ pm/V have been found [6]. The largest tensor element χ_{zzz} we obtain is identical within the experimental error to the values reported for ZnO single crystals and therefore exceeds the $\chi^{(2)}$ of traditional nonlinear crystals like BBO and KDP [7]. Second-harmonic generation (SHG) has been detected before in polycrystalline ZnO films grown on a variety of substrates by a multitude of techniques [6,8]. But, no previous realization would integrate easily with complex topology as encountered on a photonic chip and still exhibit maximal $\chi^{(2)}$ nonlinearity. Here, we use ALD that indeed interfaces very well with photonic waveguides [9].

The thin films studied here are deposited on glass (BOROFLOAT® 33, 500 µm thickness) using a homebuilt ALD setup with a base pressure of 10^{-6} mbar. Experiments are performed on two different samples: (I) 39.1 nm ZnO on glass, and (II) 36.7 nm ZnO on 6 nm Al_2O_3 on glass. The thicknesses are determined through x-ray reflectivity measurements. An Al_2O_3 seed layer is used in sample (II) because it has been shown to promote (002) orientation of the ZnO crystallites (c-axis perpendicular to the substrate) and improve $\chi^{(2)}$ [5,10]. The Al_2O_3 layer is deposited via thermal ALD at a substrate temperature of 120°C (from trimethylaluminium and water, both for 5 s at 5×10^{-3} mbar). ZnO deposition is done at a substrate temperature of 300°C by PE-ALD (using 5 s diethyl zinc at 5×10^{-3} mbar and 10 s oxygen plasma at 10^{-2} mbar). The O_2 plasma is generated at an RF power of 200 W and a frequency of 13.56 MHz.

The $\chi^{(2)}$ tensor elements of ZnO are determined and verified by SHG experiments using two different setups operating at a fundamental wavelength of 980 nm (100 fs pulses, repetition rate of 80 MHz) and 800 nm (165 fs pulses, repetition rate of 80.5 MHz) respectively. In the first setup light at the fundamental and second-harmonic (SH) frequency is p-polarized and the SH power $P_{2\omega}$ is recorded as a function of the angle of incidence ϑ (with respect to substrate normal). The setup and model are explained in more detail in [4]. In the second setup the SH power $P_{2\omega}$ (p-polarized SH waves) is measured as a function of angle of incidence ϑ for p- and s-polarized input waves at the fundamental frequency. More information about the setup and theoretical model can be found in [3,5]. Measurements are calibrated with a Y-cut quartz plate assuming $\chi_{XXX} = 0.6$ pm/V [7].

The SHG measurements for the first setup at a fundamental wavelength of 980 nm are shown in Fig. 1 (a). The fitting results are summarized in Table 1. As we are operating far from material resonance we expect $\chi_{xxz} \approx \chi_{zxx}$. The measurements on the setup from [3,5] at a wavelength of 800 nm are shown in Fig. 2. The fitting results are

summarized in Table 2. SHG measurements for both p- and s-polarized input waves allow χ_{xxz} and χ_{zxx} to be determined separately. The obtained χ_{xxz} and χ_{zxx} are not equal which can be related to the SH frequency that approaches the band gap. As such, resonant enhancement can play a role and Kleinman symmetry will no longer be valid. The main error source in both setups is the systematic error on the angle of incidence.
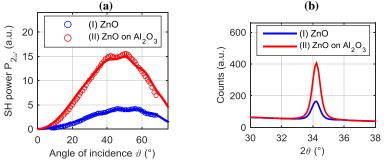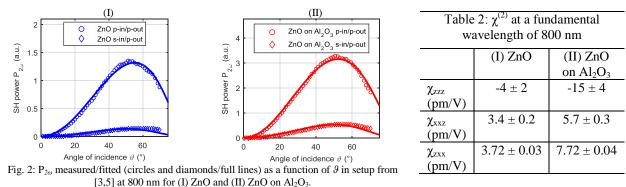

Fig. 1: (a) $P_{2\omega}$ measured/fitted (circles/full lines) as a function of ϑ in setup from [4] at 980 nm.
(b) XRD θ-2θ scan for sample (I) and (II) using Cu Kα radiation.

Table 1: $\chi^{(2)}$ at a fundamental wavelength of 980 nm

	(I) ZnO	(II) ZnO on Al_2O_3
χ_{zzz} (pm/V)	-4 ± 2	-14 ± 5
$2\chi_{xxz}+\chi_{zxx}$ (pm/V)	5.9 ± 0.5	13.1 ± 0.9

Fig. 2: $P_{2\omega}$ measured/fitted (circles and diamonds/full lines) as a function of ϑ in setup from [3,5] at 800 nm for (I) ZnO and (II) ZnO on Al_2O_3.

Table 2: $\chi^{(2)}$ at a fundamental wavelength of 800 nm

	(I) ZnO	(II) ZnO on Al_2O_3
χ_{zzz} (pm/V)	-4 ± 2	-15 ± 4
χ_{xxz} (pm/V)	3.4 ± 0.2	5.7 ± 0.3
χ_{zxx} (pm/V)	3.72 ± 0.03	7.72 ± 0.04

The use of a 6 nm Al_2O_3 seed layer clearly improves the $\chi^{(2)}$ response. An x-ray diffraction (XRD) θ-2θ measurement shows that the increase in $\chi^{(2)}$ is correlated to an increase in the (002) diffraction peak (see Fig. 1 (b)). The $\chi^{(2)}$ values are larger than those reported for thermal ALD ZnO in [5] (χ_{zzz} = -4.0 pm/V, χ_{xxz} = 1.6 pm/V and χ_{zxx} = 1.5 pm/V for an optimized ZnO/Al_2O_3 nanolaminate). We believe the improvement is related to the use of a plasma and possibly the slightly elevated substrate temperature (300°C vs 250°C) which promotes (002) orientation of the crystallites.

As can be seen in Table 1 and 2 we find identical χ_{zzz} (within experimental error) for our ZnO films at a wavelength of 980 nm and 800 nm. For the off-diagonal components the dispersion appears larger. This could be attributed to bulk and grain boundary contributions to the total SHG [6]. As the chemical bonds at grain boundaries are different from those in bulk crystal, the resonance wavelength of the grain boundary contributions will also deviate from the bulk material resonance.

Using a 6 nm Al_2O_3 seed layer we get χ_{zzz} in PE-ALD ZnO in line with bulk ZnO crystals. Our coating has also been deposited on existing low loss Si_3N_4 waveguides and it induced a limited excess loss of 3-4 dB for a waveguide of 1 cm at a wavelength of 900 nm. We therefore believe our results open the road towards on-chip, efficient Si_3N_4 based optical parametric oscillators and fast electro-optic modulators.

References
[1] E. L. Wooten *et al.*, IEEE J. Sel. Top. Quantum Electron. **6**, 69-82 (2000).
[2] M. A. Arbore and M. M. Fejer, Opt. Lett. **22**, 151-153 (1997).
[3] L. Alloatti. *et al.*, Appl. Phys. Lett. **107**, 121903 (2015).
[4] S. Clemmen *et al.*, Opt. Lett. **40**, 5371–5374 (2015).
[5] A. Wickberg *et al.*, Adv. Opt. Mater. **4**, 1203-1208 (2016).
[6] M. C. Larciprete and M. Centini, Appl. Phys. Rev. **2**, 031302 (2015).
[7] V. G. Dmitriev, G. G. Gurzadyan and D. N. Nikogosyan, *Handbook of Nonlinear Optical Crystals* (Springer, Berlin, 1999), 3rd edn.
[8] G. Wang *et al.*, Appl. Phys. Lett. **80**, 401-403 (2002).
[9] A. Khanna *et al.*, Opt. Express **22**, 5684-5692 (2014).
[10] H. Mohseni and T. W. Scharf, J. Vac. Sci. Technol. A **30**, 01A149 (2012).